

---

## Array formation in nano-colloids: Theory and experiment in 2D

---

William M. Gelbart,\*<sup>a</sup> Richard P. Sear,<sup>b</sup> James R. Heath<sup>a</sup> and Stephanie Chaney<sup>a</sup>

<sup>a</sup> Department of Chemistry and Biochemistry, University of California at Los Angeles, 405 Hilgard Avenue, Los Angeles, CA 90095-1569, USA

<sup>b</sup> Department of Physics, University of Surrey, Guildford, Surrey, UK GU2 5XH

Received 8th December 1998

We discuss theoretical and experimental aspects of the array formation of nano-colloids in two-dimensional (2D) situations. In particular, we treat metal nanocrystals which have been passivated by surfactant monolayers and then deposited on the free surface of water. Their self-organization properties follow from the fact that the relevant interparticle attractions do not greatly exceed thermal energies, thereby allowing for equilibrium structures to form and to evolve reversibly as a function of temperature and concentration. In the case of large enough metal cores, spatially-modulated phases arise because of long-range repulsions between particles; for smaller cores, the interactions are highly directional, giving rise to linear chain structures at low concentrations and to extended networks at higher densities.

---

We have been interested for the past several years in the self-assembly properties of colloidal solutions of metal nanocrystals passivated by surfactant. Unlike most work in the nanoparticle field, our focus has been on the equilibrium statistical mechanical features of these suspensions, rather than on the optical or electronic characteristics of the individual particles.<sup>1</sup> Much of our interest is spurred by the fact that the attractions between particles are not too large compared to thermal energies ( $k_B T$ ), thereby allowing the system to “anneal” into equilibrium configurations. This fact in turn follows from the small (*i.e.*, few nanometers) size of the polarizable cores of the particles and from their being separated through chemisorbed monolayers by large enough distances (again, nanometers), even at closest approach. Instead of being concerned with any details of the specific metals or surfactants involved, we focus on the generic properties of a suspension of weakly interacting particles, in particular, their preferences for different patterns of structural organization and long-range ordering under a wide variety of physical conditions.

In the present paper we start in Section I with a brief discussion of the spatial structures developed spontaneously by metal nanoparticles, which are deposited on solid substrates under sub-monolayer conditions. Section II then treats, in significantly greater detail, the array formation observed for these same particles when they are deposited instead on the free surface of water. The concluding discussion in Section III emphasizes the many open questions which remain and includes some speculation about the microscopic origins of the interactions acting between particles.

Before proceeding further it is important to introduce the generic particles in question, in particular, how they are made and what they look like. There is, of course, a huge literature on silver and gold nanocrystals stabilized by alkylthiols and alkylamines, see recent papers and reviews.<sup>2</sup> One of the most widely used syntheses involves<sup>3</sup> the borohydride reduction of aqueous gold chloride salts, in the presence of alkylthiol and the phase-transfer (water to organic solvent) agent tetraoctylammonium. As shown in earlier work,<sup>4</sup> the size of the particles can be controlled by

varying the mole ratio of thiol to metal, *i.e.*, by fixing the surface-to-volume ratio. Indeed we have argued that in many cases the dispersion of nanocrystals is in thermodynamic equilibrium, much like the droplets in a water-in-oil micro-emulsion, say, where the role of surfactant is to lower the interfacial energy per “particle” to the point where it is no longer large compared to  $k_{\text{B}}T$ . In the nanocrystal case, this dramatic lowering of surface energy is associated with the fact that the gold–thiol bond strength is comparable to that of gold–gold interactions.

For our present purposes, we will consider the following “picture” for the structure of the nanoparticles. A spherical metal core is surrounded by a monolayer of alkylthiol chains. The interface is assumed to be essentially saturated, *i.e.*, the metal surface is covered by the “maximum” number of surfactant molecules: each thiol occupies the same area as it does in self-assembled monolayers on bulk gold surfaces. This assumption leads to a simple prediction, based solely on geometry, for how the number of surface-metal atoms per thiol increases with particle size, in particular, from about 2 to 3 as one proceeds from 6 nm metal diameter, say, to a bulk (planar) surface, in good agreement with results from detailed molecular dynamics simulations.<sup>5</sup> In the discussion below we shall use  $L$  to denote the length of the surfactant chains, and consider a factor-of-two range of  $L$ , corresponding to carbon numbers varying from 9 to 18; we write the area per thiol as  $\pi f^2$ , and keep  $f$  constant as we move from one combination of metal diameter ( $2R$ ) and surfactant chain length ( $L$ ) to another. It turns out that we will make distinctions between “small” and “large” particles, both in Section I where we treat array formation on solid substrates, and in Section II where we focus on pattern formation at the air/water interface. In the former case it will be the overall particle size that is important, whereas in the latter it is the ratio of  $R$  to  $L$ .

## I Nanoparticles on solid substrate

Our primary interest in this paper is the spontaneous formation of patterns of nanoparticles at the free surface of water, as discussed in Section II. Nevertheless, it is useful to present briefly the rather different situation that arises when the particles are deposited instead on a solid substrate. Consider a small ( $\mu\text{l}$ ) drop of a dilute (about  $10^{14}$  particles  $\text{ml}^{-1}$ ) solution of gold–thiol particles in hexane, with their metal diameter about 6 nm. Consider also a TEM substrate that consists of a square millimetre of fine copper mesh covered by amorphous carbon. When the drop of solution is placed on the grid, and the solvent evaporates, one is left with a sub-monolayer of particles. If the particles are “large enough”, *e.g.*, 5–6 nm diameter in the case of gold  $\text{C}_{12}$  thiols, one typically sees annular rings in the TEM imaging, *i.e.*, isolated circles, several particles thick and with a radius roughly ten times larger than the annular width. As stressed in our earlier work,<sup>6</sup> the entire square millimetre of grid shows this one size of ring. More explicitly, for any given solution, *i.e.*, particle size, concentration, and solvent, all rings have essentially the same diameter and annular width. This phenomenon was argued to derive from the following considerations.

Even though the solvent (hexane, toluene, *etc.*) wets the substrate (amorphous carbon), once it has evaporated below a certain thickness the thin film becomes unstable with respect to the nucleation and growth of holes. Basically, the holes reflect the film’s effort to increase its thickness in order to satisfy the demands of the disjoining pressure, whose contribution to the free energy per unit area has the form  $A_{\text{H}}/t^2$ , where  $t$  is the film thickness and  $A_{\text{H}}$  is the Hamaker constant relevant to liquid solvent layer between vapor and wetting solid substrate. This driving force is resisted by the positive spreading coefficient,  $S$ , describing the wetting of the substrate by the solvent:  $S = \gamma_{\text{sv}} - (\gamma_{\text{sl}} + \gamma)$ , where  $\gamma$  is the liquid/vapor interfacial tension and  $\gamma_{\text{sv}}(\gamma_{\text{sl}})$  the corresponding value for the solid/vapor (solid/liquid) interface.  $t_{\text{e}} \approx (A_{\text{H}}/S)^{1/2}$  is the equilibrium thickness resulting from the compromise between these competing tendencies of thinning, wetting film.<sup>7</sup> Accordingly, when the film thins down to thicknesses just below  $t_{\text{e}}$ , holes open up and grow, pushing solvent and particles out toward the bulk film of solution. But the particles can only be moved if the force acting on them is sufficient to overcome the friction arising from their attraction to the substrate. And the force acting on the hole rim increases linearly with the size of the hole, whereas the number being swept out by the hole area increases quadratically. It follows that there will be a limiting hole size at which point its contact line becomes pinned due to particle–

substrate interactions: the resulting hole size will be inversely proportional to particle concentration, consistent with preliminary experimental observations.

It turns out, as a consequence of the above scenario, that if the particle concentration is sufficiently low the contact lines of the holes will not be pinned before the growing holes “percolate”. Then, instead of the annular rings, one expects to see compact domains of particles, due to their having been pushed into the interstices of the percolating holes. We argue elsewhere<sup>8</sup> that faster evaporation can also lead to percolation of holes and hence to loss of the annular ring structures. Finally, it is also possible that changing the size of the particles would constitute another way to favor compact domain formation. In particular, smaller particles would more easily have their static friction overcome as long as the force attracting particles to the substrate increases faster than quadratically with their size. Then the critical (pinning) hole size could become larger than the average distance between holes and their percolation would lead to compact domains, such as those analyzed by us earlier.<sup>9</sup> In that case, when the size distribution is polydisperse, the larger particles are found in the center, with progressively smaller particles appearing as one proceeds radially outward. This size segregation has been explained previously in terms of the size-dependent dispersional interactions between particles, *i.e.*, the biggest particles crystallize first as the solvent evaporates (concentration increases), with the smaller ones following suit.

## II Nanoparticles at the air/water interface

For the rest of our discussion, we focus on the case of nanoparticles being deposited on the free surface of water, in a Langmuir trough. In both situations described below we are concerned with demonstrating that the spatial patterns formed by the particles interacting in 2D correspond to equilibrium structures. For example, we attempt to produce a particular array from at least two, totally different, routes, making more plausible the conclusion that, for a given type of particle (and hence interparticle potential), the array formation depends only on concentration (and temperature, of course, which is always  $T_{\text{room}}$ ).

The first route consists in depositing a single drop of dilute nanoparticle solution on the surface of water. One sees the solvent evaporate within seconds, and the particles form a sub-monolayer along one of the edges or corners of the trough. Transferring these particles to a TEM grid by the horizontal lift-off (Langmuir–Schaeffer) technique described elsewhere,<sup>10</sup> one sees two essentially different classes of patterns. As discussed at length in the two subsections below, whether one sees circular and stripe clusters, or linear chains and networks, depends on the nature of the particle, *i.e.*, its ratio of metal core radius  $R$  to alkylthiol thickness  $L$ . All we want to emphasize at this point is that, for a given particle, the spatial pattern formed in these single-drop deposition experiments depends only on the concentration of the solution from which it is taken.

For example, a pattern of isolated circular clusters of close-packed particles results from depositing a single drop of a  $0.1 \text{ mg ml}^{-1}$  solution of 4–6 nm diameter silver– $\text{C}_{12}$  alkylthiol particles in hexane. One sees the same thing if one successively deposits many more drops of the same solution before transferring the particles to a TEM grid. Indeed, one can fill up the entire trough by successive depositions, and the same images will be obtained. “Fill up” here does not mean at full-monolayer coverage, but rather at the same coverage observed locally in the single-drop case. The only way in which new patterns arise is when one begins to compress the film once enough drops have been deposited to “fill up” the trough, or when one deposits a drop from a higher concentration solution. If, for example, we take a drop of these same 4–6 nm particles but now from a solution whose concentration is  $0.5 \text{ mg ml}^{-1}$ , one sees many-particle-thick stripes, instead of circular clusters. But the stripe pattern can also be obtained directly from the circles, *i.e.*, for the deposition of  $0.1 \text{ mg ml}^{-1}$  particles, if one compresses the system of circles. Furthermore, expansion of the system can be shown to give back the circle pattern. Similar arguments can be made in the case of the smaller metal core/longer alkylthiol particles, which give rise to linear chain and then extended networks patterns, *i.e.*, the characteristic structure of the array formed by a given system of particles at a given temperature is again a function only of concentration.

So we see the role of increasing concentration is to either drive the 2D array from circles to stripes (and ultimately to hexagonal close-packed structures), or from linear chains to space-filling networks (and then to amorphous close-packed configurations). These two scenarios correspond to two different regimes for the ratio of metal core radius to surfactant length, as explained below.

## A Large particles

What we mean by “large” particles here is simply that the metal core radius  $R$  is significantly greater than the thickness  $L$  of the surfactant monolayer. The condition  $R \gg L$  results (see Section III) in the particles interacting through spherically symmetric forces whose attractive range is shorter than that of the repulsions, leading to size-limited condensates at low concentrations, as discussed immediately below. This condition is closely related to the small  $V_e$  condition discussed earlier by Heath *et al.*<sup>10</sup>  $V_e$  was introduced as an “excess volume” per adsorbed surfactant, essentially measuring the “free space” (beyond the molecular volume  $f^2L$ ) available to each ligand as it extends from the surface of the metal core; recall that  $f^2$  is the area per thiol.  $R \gg L$  means that there is little splay and hence little excess volume associated with the adsorbed chains. In the case of the particles under discussion here, this condition corresponds, say, to  $R > 3$  nm for  $C_{12}$  chains.

We argue that the essentially monodisperse, circular, islands formed when a low-concentration drop of “large” particles is deposited on the free surface of water are a direct consequence of pair potentials between particles that are spherically symmetrical and whose attractive interactions are shorter ranged than their repulsions. More explicitly, at short distances the particles attract each other and so they condense (at the low temperatures relevant to the experiments, see below) into close-packed structures. But once these condensates reach a size comparable to the (longer) range of the repulsive interactions, the energy per particle begins to increase because of larger numbers of pairs of particles separated by distances at which the potential is positive. Indeed, we have shown that Monte Carlo simulations with pair interactions of this kind give the same result. We happen to have chosen<sup>11</sup> a potential  $u(r)$  which can be written as a sum of exponential function of interparticle distance  $r$ :  $u(r) = -\epsilon_a \gamma_a^2 \exp(-\gamma_a r) + \epsilon_r \gamma_r^2 \exp(-\gamma_r r)$ . Here  $\epsilon_{a(r)} > 0$  and  $\gamma_{a(r)}^{-1} > 0$  are the strengths and ranges of the attractive (and repulsive) interactions, respectively. The inequality  $\gamma_r^{-1} > \gamma_a^{-1}$  simply guarantees that the repulsive term is longer ranged than the attraction. Otherwise, with interaction strengths  $\epsilon_a$  and  $\epsilon_r$  being comparable, the particular form of the potential is of little consequence. Equilibrated configurations at low area fraction show a phase of circular clusters whose size is essentially determined by the range  $\gamma_r^{-1}$ . At higher area fractions the preferred pattern is one of stripes, in agreement with the experimentally observed structure mentioned above, which arose spontaneously following deposition of a drop of the same “large” particles but from a solution of higher concentration. Finally, at still higher concentrations, one sees hexagonally close-packed structures, both experimentally and in simulation. We stress that this same sequence of structural evolution, from circles to stripes to bulk crystalline domains, is observed upon slow compression (and then in reverse, when followed by expansion) of a “full” monolayer of particles from a dilute solution.

Additional indication that these spatially modulated structures correspond to equilibrium states of the system comes from systematic calculations by Hurley and Singer on the “dipolar lattice gas”.<sup>12</sup> A great deal of earlier work addressed the problem of domain structures in ferromagnetic thin films, where magnetic dipoles compete with shorter-ranged attractions to give patterned phases, and in Langmuir monolayers where electric dipoles give rise similarly to circular and stripe domains of molecules in 2D.<sup>13</sup> McConnell<sup>14</sup> focused attention, in particular, on the effects of competing length scales in the case of oriented (hence repulsive at large distance, interacting as  $1/r^3$ ) dipoles at the air/water interface. His calculations are done at the continuum level, pitting a line tension, deriving from the short-ranged attractions, against the dipolar “bulk” energy; interactions between domains are explicitly included, and a transition from circles to stripes is predicted upon increase in concentration. In the work of Hurley and Singer on the other hand, the particles are treated within the context of a lattice gas Hamiltonian:  $H = -J \sum_R \sum_{R'} n_R n_{R'} + A \sum_R \sum_{R'} (n_R n_{R'}) / |R - R'|^3 - \mu \sum_R n_R$  ( $n_R$  is equal to 1 if site  $R$  is occupied, and 0 otherwise). The first term describes the short-range attractions of strength  $J > 0$ , and hence involves only nearest-neighbor sites, whereas the second, dipolar, term with strength  $A$  includes repulsions between all pairs;  $\mu$  is the chemical potential which controls the concentration of particles. The preferred states of spatial modulation are then explored *via* Monte Carlo simulation as a function of temperature ( $\leftrightarrow J$ ), area fraction ( $\leftrightarrow \mu$ ) and particle “type” (the ratio  $A/J$ ). A wide range of structures and phase behaviours are obtained, including the transition from circles to stripes upon increase in concentration.

It is interesting to remark here on analogies with structural evolution in micellized surfactant

solutions. In this latter case, the physical origin of the competing interactions between particles is more subtle. Indeed, the “particles” themselves are aggregates, micelles, consisting of a large number of individual molecules. The molecules have self-assembled into micelles in order to satisfy the hydrophobic effect’s requirement that water be shielded from the alkyl chains of the surfactants; all the hydrophilic (dipolar and/or charged) head groups sit at the micelle/water interface. But many different curvatures are possible, depending on details of the individual amphiphilic molecule involved; accordingly, at the c.m.c. one sees either globular (“spherical”), rodlike (cylindrical) or planar (bilayer) aggregates. And it is possible to formulate the basic physics of this structural organization in lattice model language, involving ferromagnetic (attractive) nearest-neighbor interactions and anti-ferromagnetic (repulsive) next-nearest-neighbor interactions,<sup>15</sup> in a manner reminiscent of the dipolar lattice gas, say, described above. Again the idea is that the “condensates” (micelles!) are limited in size, and that their preferred shape progresses from one curvature to a lower one as the overall concentration is increased. This fundamental result is related to the geometric fact that objects of higher curvature pack less efficiently than ones with lower curvature. Alternatively put, the average distance between spheres, for example, is larger than that between aligned cylinders at any given volume fraction of material; hence the repulsive energy of interaction is greater in the former case than in the latter.

## B Small particles

Recall that by “small” we mean that the radius of the metal core is smaller than the thickness of the passivating monolayer. This is the situation obtained, say, for 4 nm metal diameters and  $C_{18}$  alkyl thiols. Suppose a microlitre drop of a dilute ( $\ll \text{mg ml}^{-1}$ ) hexane solution of these particles is deposited on the Langmuir trough. Upon evaporation of the solvent, the particles are seen again to cluster along a small portion of the edge of the trough. Transferring the particles to a TEM grid by the technique described in Section IIA, single-particle-thick chains and rings appear overwhelmingly to be the preferred mode of spatial organization. Again, as with the competing interactions (spherically symmetric attractions and longer-ranged repulsions) featured in the case of “large” particles in the preceding section, we do not know the microscopic origin of the interactions which lead to the linear-chain structures. We speculate a little about them in Section III, but for the present purposes we proceed as follows. The linear chains indicate clearly that, for whatever reasons, the particles strongly prefer to associate with two, and only two, neighbors. At low concentrations (area fractions), the system can easily accommodate this preference for two-fold coordination. The question immediately arises: what are the consequences of higher concentrations on the spatial organization of particles? More explicitly, do the isotropic distributions of linear chains which characterize the low-density structure evolve *via* space-filling networks of branched chains or into the amorphous close-packed arrays which appear at high area fractions?

To treat the evolution of spatial structures in the small-particle systems described above, we find it useful to consider the “multiple bonding site” intermolecular potential models introduced for the study of phase equilibria in associating liquids.<sup>16</sup> The original motivation for these potentials was to understand the nature of hydrogen bonding in simple molecular liquids, where low-fold “coordination” arises naturally, “on top of” the usual short-range repulsions and dispersive attractions. In the case of HF, for example, it is reasonable to impose two sites (for H and F) on each spherically symmetric particle, and add the resulting interaction effects to the hard core plus long range attraction structure and thermodynamics. In the present case, a model of this kind becomes still more interesting because our system is “lyotropic” rather than “thermotropic”, *i.e.*, the concentration is varied over several orders of magnitude rather than essentially corresponding to a fixed, neat-liquid value. Accordingly, the linear chains of particles, which dominate the structure at low concentration, can be interpreted more literally than in the neat-liquid case where they constitute a highly interconnected network superimposed on the usual liquid-state structure. And of course, because the nanoparticle system is two-dimensional, with configurations imaged directly in real space, there are much more unambiguous distinctions between linear chains, space-filling networks, and close-packed structures.

We specify the pair potential energy of interaction, as follows.

$$u(r) = -\varepsilon, \text{ if cones of Fig. 1 overlap with } r \geq \sigma; \quad \infty, \text{ if } r < \sigma; \quad \text{and } 0, \text{ otherwise.} \quad (1)$$

Here  $r$  is the distance between centers of particles, and  $\phi_i$  is the angle formed by the line between centers and the line connecting the two sites of the  $i$ th particle, as shown in Fig. 1. Note that  $\sigma$  specifies the hard core diameter of the particles, and that “bonding” (lowering of the energy by  $\epsilon$ ) occurs only if the distance between particles is less than  $r_c$ , which is generally taken to be 10–50% larger than  $\sigma$ ; both of the angles  $\phi_i$  must also be less than the cut-off value  $\phi_c$ .

To get a feeling for the effects of this simple, directional, potential, we show in Fig. 2(a) a typical configuration from an equilibrated sample of 900 particles at an area fraction of 0.1. These results correspond to an  $N,V(A!)$ ,  $T$  Monte Carlo simulation at a temperature  $k_B T/\epsilon = 0.125$ , and with

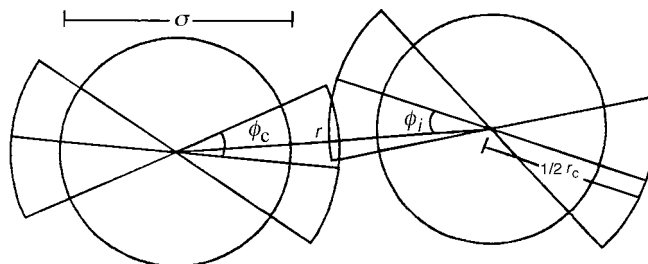


**Fig. 1** Shown here are the coordinates  $r$  and  $\phi_i$ , cut-off angle  $\phi_c$  and lengths  $\sigma$  and  $r_c$ , in terms of which the two-site potential given by eqn. (1) is defined.

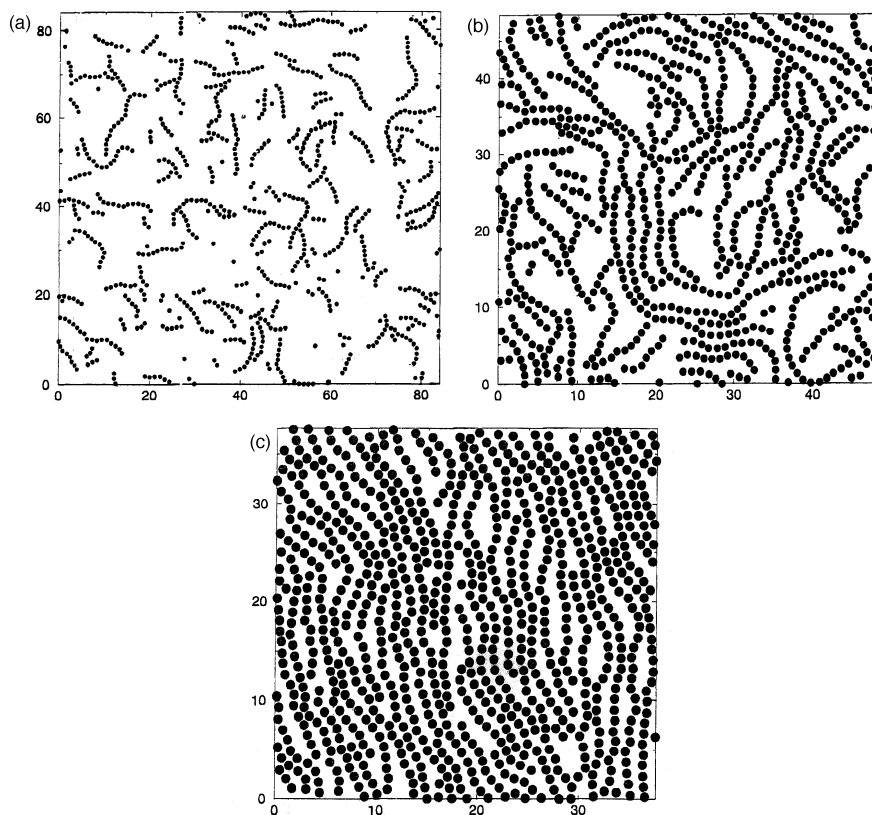


**Fig. 2** Typical configurations in equilibrated systems of two-site particles [see eqn. (1) and Fig. 1] at area fractions  $\eta = 0.1$  (a), 0.3 (b) and 0.5 (c), from a Monte Carlo simulation at a temperature  $k_B T/\epsilon = 0.125$ , and with distance and angle cut-off values of  $r_c = 1.2\sigma$  and  $\phi_c = 0.42$ , respectively. The  $x$ - and  $y$ -axes are labeled in units of  $\sigma$ .

distance and angle cut-off values of  $r_c = 1.2\sigma$  and  $\phi_c = 0.42$ , respectively. At a higher concentration, say, 0.3, the linear chains are still isotropically distributed, but they are significantly longer on average, as seen in Fig. 2(b). In fact, one can derive approximate analytical expressions for the average length of chain or, equivalently, the average fraction of sites  $F$ , which are involved in bonding; the average length, in units of  $\sigma$ , is given by the reciprocal of  $1 - F$ . More explicitly,  $F$  can be written as

$$1 - F = 2/\{1 + \sqrt{1 + 8\rho K g_c e^{\epsilon/kT}}\} \quad (2)$$

Here  $\rho = N/A$  is the total particle density and  $K = (r_c^2 - \sigma^2)(\phi_c^2/\pi)$  is the “bonding area” associated with a pair of particles;  $g_c$  is the value of the hard-disk radial distribution function at contact, *i.e.*, at  $r = \sigma$ .

The chains in Fig. 2(a) reflect the non-zero persistence length,  $l_p$ . In continuous elastic space-curve models, for example, one can ascribe an exponential form  $e^{-s/l_p}$  to the decay of the autocorrelation function  $\langle \theta(s)\theta(s+t) \rangle$  where  $\theta(s)$  is the angle associated with the tangent vector at the point  $s$  along the curve contour. Equivalently, we can calculate here the average value  $\langle \cos \theta_n \rangle$  of the cosine of the angle between the  $n$ th bond in a chain and the first. The result is shown by the circles in Fig. 3. At higher values of concentration, the function is seen to decay more slowly (see the squares in Fig. 3, corresponding to an area fraction of  $\eta = 0.3$ ). Here the “extra” persistence is due to the interactions between chains and the fact that they begin to align locally in order to pack more efficiently. At still higher concentrations, in fact, the system undergoes a thermodynamic transition to a nematic state in which there is a macroscopically preferred direction for the alignment of bonds. This effect is seen in the  $\eta = 0.5$  configuration of Fig. 2(c) and in the diamond curve of Fig. 3.

It is interesting to note the similarity between the linear chains in Fig. 2(a) and the configurations reported for dipolar hard disks in 2D.<sup>17</sup> In this latter case the two-fold coordination arises from the preference for a pair of dipoles to lie “head-to-tail”, rather than alongside one another with opposite directions, if they are constrained (by spherically symmetric hard cores) to have their centers a certain distance apart. At low densities it can be shown that the formation of chains virtually saturates the interaction between dipolar disks, thereby emasculating the driving force for condensation to a liquid phase.<sup>18</sup> Instead, the linear chains remain stable, upon decrease in temperature, much as in the two-site disk model described above.

At higher concentrations, see the  $\eta = 0.5$  case shown in Fig. 2(c), where nematic order has set in, the persistence length is no longer a relevant scale; indeed, as seen in the diamond curve of Fig. 3,  $\langle \cos \theta_n \rangle$  never decays to zero because of the long-range orientational order. As pointed out earlier by Odijk,<sup>19</sup> the relevant length is now the contour distance “traveled” by a chain before it makes

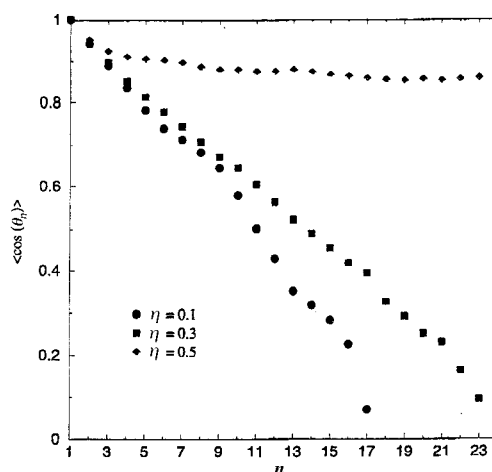


**Fig. 3**  $\langle \cos \theta_n \rangle$  vs.  $n$  for the equilibrated systems in the simulations of Figs. 2(a), (b) and (c).  $\theta_n$  is the angle between the  $n$ th and 1st “bonds” in a linear chain.

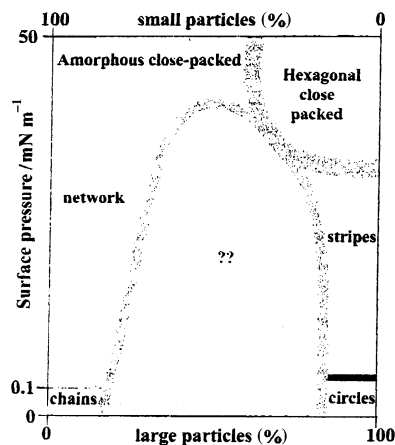


**Fig. 4** Schematic phase diagram indicating dependence of spatial patterns discussed in the text on surface pressure (density) and composition (fraction of small and large particles). All boundaries are highly approximate; ?'s in center refer to the “eggs” and mixed lamellae described in Section III.

contact through thermal fluctuations with a neighboring chain having the same average alignment. This “deflection” length  $\lambda$  is smaller than the persistence length  $l_p$  by a factor of  $\alpha$ , where  $\alpha$  ( $\gg 1$ ) measures the reciprocal width of the orientational distribution defining the nematic state:  $\langle \theta^2 \rangle \approx 1/\alpha$ .

But to treat more thoroughly the higher concentration states of our system, we need to consider the network and close-packed structures in which three- and higher-fold coordination arise as the particles are crowded together at high area fractions. Indeed, one can see this kind of structural evolution, even within the two-site interaction model defined by eqn. (1), by only slightly increasing the angular cut-off  $\phi_c$ , just beyond its critical value of  $\sin^{-1}(\sigma/2r_c)$ . Probably it is more illustrative, however, to introduce a two-species system in which one type of particle has two sites, and the other has three; the former strongly prefers two-fold coordination, while the latter is primarily involved in three-fold vertices. Introducing chemical potentials for each then allows most naturally for cross-over from linear-chain to extended-network configurations upon increase in overall concentration. Alternatively, one can define an interparticle attraction which allows for up to, say, six-fold coordination, but which associates an increasingly large energy penalty per bond as progressively more than two bonds per particle are involved. Both of these approaches are presently being pursued.

### III Conclusion

Here we discuss briefly the little that can be said at present about the physical origins of the types of interactions invoked above to treat our “large” and “small” nanoparticles on the surface of water. We also speculate on a novel phase diagram for this system.

In the case of “large” particles, we have assumed that they interact through spherically symmetric potentials. This is consistent with the condition  $R \gg L$ , *i.e.*, the metal core radius is much larger than the alkyl layer thickness, so that the flexible chains are minimally splayed. Each nanoparticle on water involves an area several nanometres square, over which the surface of water is in contact with a hydrocarbon monolayer. While it is not known how water is “reconstructed” at such an interface, it is clear that the net dipole moment associated locally with each such region is necessarily different from that at the free surface of water. Hence there should be a long-ranged, dipole–dipole, repulsion between particles, and very rough estimates<sup>11</sup> suggest that this interaction can indeed be significant at distances many times larger than the particle diameter.

For “small” particles, on the other hand,  $R \ll L$  implies a high positive curvature and large degree of splay in the adsorbed monolayers; this suggests that chains on neighboring particles will mutually interdigitate in order to “dissolve” in each other. It follows that the interparticle poten-

tial should be highly directional and non-pairwise additive; once the chains on each side of an  $R \ll L$  particle are tied up in interaction with a pair of apposite neighboring particles, there is little of the monolayer available for strong interdigitation with a third particle. As far as we are aware there is no theory at present that addresses this effect; it would be interesting to apply recent formulations of adsorbed chain statistics to this particular geometry.

Finally, we remark on directions for future work which involve a more systematic exploration of the phase behavior of the spatially modulated patterns formed by alkyl-saturated metal nanoparticles on water. Fig. 4 shows a highly speculative and schematic view of the problem. The vertical axis denotes concentration (or lateral pressure in the Langmuir trough), while the horizontal axis refers to particle size and polydispersity. At the right end of the horizontal axis lie the systems of "large" particles; as we move up in concentration the system evolves from circular clusters to stripes to hexagonal crystalline structures, as discussed in Section IIA. Similarly, at the left end lie the monodisperse "small" particles, which first form linear chains, then extended networks, and then amorphous close-packed structures as they are forced to organize at progressively higher densities. In between, where we have, say, a mixture of "large" and "small" particles, what do we expect? In fact, preliminary experimental measurements indicate a surprising and striking result. At low densities the mixture self-assembles into "sunny-side-up" egg structures in which the large particles are hexagonally close-packed as the "yolk" and the small particles surround them as the "white" in an extended network of chains. At higher densities these complex clusters evolve into lamellar stripes in which the large and small particles alternate in regions whose lengths are comparable to the stripe widths. Clearly, much more work needs to be done before these rich and beautiful systems are properly explored and understood.

## Acknowledgements

We thank Sung-Wook Chung for his on-going contributions to the experimental program discussed above. This work has been supported by the American Chemical Society Petroleum Research Fund (grant #31797-AC9) and by the Office of Naval Research (grant #N00014-98-1-0422).

## References

- 1 For a concise review of optical and electronic properties of metal nanocrystals, see C. P. Collier, T. Vossmeyer and J. R. Heath, *Ann. Rev. Phys. Chem.*, 1998, **49**, 371.
- 2 M. J. Hostetler and R. W. Murray, *Curr. Opin. Colloid Interface Sci.*, 1997, **2**, 43; C. S. Weisbecker, M. V. Merritt and G. M. Whitesides, *Langmuir*, 1996, **12**, 3763; R. L. Whetten, J. T. Khoury, M. M. Alvarez, S. Murthy, I. Vezmar, Z. L. Wang, C. L. Cleveland, W. D. Luedtke and U. Landman, *Adv. Mater.*, 1996, **8**, 428.
- 3 M. Brust, M. Walker, D. Bethell, D. J. Schiffrin and R. Whyman, *J. Chem. Soc., Chem. Commun.*, 1994, 801.
- 4 D. V. Leff, P. C. Ohara, J. R. Heath and W. M. Gelbart, *J. Phys. Chem.*, 1995, **99**, 7036.
- 5 W. D. Luedtke and U. Landman, *J. Phys. Chem.*, 1996, **100**, 13323.
- 6 P. C. Ohara, J. R. Heath and W. M. Gelbart, *Angew. Chem., Int. Ed. Engl.*, 1997, **36**, 1077.
- 7 F. Brochard-Wyart, J. M. di Meglio, D. Quere and P. G. de Gennes, *Langmuir*, 1991, **7**, 335.
- 8 P. C. Ohara and W. M. Gelbart, *Langmuir*, 1998, **14**, 3418.
- 9 P. C. Ohara, D. V. Leff, J. R. Heath and W. M. Gelbart, *Phys. Rev. Lett.*, 1995, **75**, 3466.
- 10 J. R. Heath, C. M. Knobler and D. V. Leff, *J. Phys. Chem. B*, 1997, **101**, 189.
- 11 R. P. Sear, S. W. Chung, G. Markovich, W. M. Gelbart and J. R. Heath, *Phys. Rev. E, Rapid Commun.*, in the press.
- 12 M. M. Hurley and S. J. Singer, *J. Phys. Chem.*, 1992, **96**, 1938.
- 13 See review given in M. Seul and D. Andelman, *Science*, 1995, **267**, 476.
- 14 See, for example, H. M. McConnell, *J. Chem. Phys.*, 1990, **94**, 4728.
- 15 See review in G. Gompper and M. Schick, *Self-Assembling Amphiphilic Systems, Vol. 16, Phase Transitions and Critical Phenomena*, ed. C. Domb and J. L. Lebowitz, Academic Press, London, 1994.
- 16 G. Jackson, W. G. Chapman and K. E. Gubbins, *Mol. Phys.*, 1988, **65**, 1, and references cited therein.
- 17 J. J. Weis, *Mol. Phys.*, 1998, **93**, 361.
- 18 R. P. Sear, *Phys. Rev. Lett.*, 1996, **76**, 2310.
- 19 T. Odijk, *Polym. Commun.*, 1985, **26**, 197; T. Odijk, *Macromolecules*, 1983, **16**, 1340.